Automatica 123 (2021) 109352

Contents lists available at ScienceDirect

Automatica

journal homepage: www.elsevier.com/locate/automatica

Stochastic stability analysis for Vehicular Networked Systems with State-dependent bursty fading channels: A self-triggered approach ☆

Bin Hu

Department of Engineering Technology, Old Dominion University, Norfolk, VA 23529, United States

ARTICLE INFO

Article history:
Received 10 March 2019
Received in revised form 6 June 2020
Accepted 29 September 2020
Available online 16 November 2020

Keywords:
Stochastic stability
Networked control systems
State-dependent fading channel
Self-triggered control

ABSTRACT

Vehicular Networked Systems (VNS) are mobile ad hoc networks where vehicles exchange information over wireless communication networks to ensure safe and efficient operation. It is, however, challenging to ensure system safety and efficiency as the wireless channels in VNS are often subject to *state-dependent deep fades* where the data rate suffers a severe drop and changes as a function of vehicle states. Such couplings between vehicle states and channel states in VNS thereby invalidate the use of separation principle to design event-based control strategies. By adopting a *state-dependent fading channel model*, this paper presents a novel self-triggered scheme under which the VNS ensures efficient use of communication bandwidth while preserving stochastic stability. Under the proposed self-triggered scheme, this paper presents a novel source coding scheme that tracks vehicle's states with performance guarantee in the presence of state-dependent fading channels. The efficacy and advantages of the proposed scheme over other event-based strategies are verified by a leader–follower example.

1. Introduction

1.1. Background and motivation

Vehicular Networked Systems (VNS) consist of numerous vehicles coordinating their operations by exchanging information over a wireless radio communication network. VNS represents one type of mobile ad hoc networks that has been deployed in a variety of safety-critical applications, such as intelligent transportation systems with Vehicle to Vehicle (V2V) communication (Papadimitratos et al., 2009), air transportation systems with Automatic Dependent Surveillance-Broadcast (ADS-B) (Park et al., 2014) and underwater autonomous vehicles with optic or acoustic communication (Akyildiz et al., 2005).

These vehicular networks, however, are often subject to *deep fades* where the data rate drops precipitously and remains low over a contiguous period of time. Such *deep fades* functionally depend on the vehicles' physical states (e.g. inter-vehicle distance, velocities and heading angles) (Cheng et al., 2007; Tse & Viswanath, 2005). Deep fades inevitably cause a significant degradation on system performance and result in safety issues, such as vehicle collisions. To maintain system stability and quality performance, VNS may require a large amount of communication resources, such as channel bandwidth, to recover the performance loss caused by deep fades. The overuse of communication resources, however, will certainly compromise the long-term operational normalcy of the system since electronic devices have limited energy. Therefore, system stability and efficiency must be jointly evaluated to ensure a successful implementation of VNS in the future.

Recent studies have shown that event-based communication scheme is an effective approach to utilize less communication bandwidth than traditional periodic method to maintain a specified system performance (Wang & Lemmon, 2011b). In an event-triggered scheme, the transmission of information only occurs when the variations of system states exceed a predefined state-dependent threshold. Recent work has shown that the system performance under such a state-dependent triggering scheme can be preserved when the communication delay or the number of consecutive packet loss is bounded (Guinaldo et al., 2012; Wang & Lemmon, 2011b). Such robustness, however, can be easily violated in VNS where a burst of delay or packet dropouts may occur with a nonzero probability. To address this issue, our prior work (Hu & Lemmon, 2014) proposed a new event-triggered scheme that ensures *almost sure stability* for VNS with a bursty fading channel. By exploring the dependence of channel conditions on vehicular states, efficient use of channel bandwidth

☆ This work was supported by the National Science Foundation under Grant CNS-1239222 and IIS-2007386. The material in this paper was partially presented at the 53rd IEEE Conference on Decision and Control, December 15–17, 2014, Los Angeles, CA, USA. This paper was recommended for publication in revised form by Associate Editor Dimos V. Dimarogonas under the direction of Editor Christos G. Cassandras.

E-mail address: bhu@odu.edu.

https://doi.org/10.1016/j.automatica.2020.109352
0005-1098/

under the event triggered scheme is achieved by increasing transmission time intervals as system states approach equilibrium. This paper extends the previous results of Hu and Lemmon (2014) in three nontrivial aspects. First, this paper generalizes the VNS structure in the prior work (Hu & Lemmon, 2014) that allows the results of this paper to be applied to a variety of realistic vehicular applications, such as the leader–follower mobile robotic system in Tanner et al. (2004) and the air traffic control system in Park et al. (2014) and Tomlin et al. (2000). Secondly, by relaxing the uniformly Lipschitz assumption on the system dynamics in our former results (Hu & Lemmon, 2014), this paper develops a more general self-triggered and encoder/decoder scheme under which four types of *stochastic stability* are ensured for VNS. More importantly, this paper provides sufficient conditions under which the VNS is *almost surely asymptotically stable*. To the best of our knowledge, these are the first set of results in the event-triggering/self-triggering community that consider almost sure stability for networked control systems. Thirdly, extensive simulation results are presented in this paper to further demonstrate the benefits and advantages of our proposed self-triggered scheme under bursty fading channels against traditional event-triggered schemes, such as Tabuada (2007), Wang and Lemmon (2009, 2011b).

Besides stochastic stability considered in this paper, (stochastic) string stability is another challenging problem that needs to be addressed to ensure ultimate success of VNS in the near future. Though a significant amount of research efforts has been devoted to this area over the past decades since the seminal paper (Swaroop & Hedrick, 1996), few results have been developed to ensure stochastic string stability for VNS under the *state-dependent fading channels* with few exceptions (Hu & Lemmon, 2015). The work in Hu and Lemmon (2015) has focused on developing a distributed switching control strategy to address the string stability issues rather than a self-triggered communication strategy considered in this paper. Other research work, such as Guo and Wang (2014) and Guo and Wen (2015), investigated both control and communication policies to ensure string stability for VNS under the assumption that fading channels are modeled as independent Bernoulli processes or Markov chains. Such channel models cannot capture the *state dependent* features in V2V communication systems as verified by recent experimental tests and results, e.g., in Cheng et al. (2007), Mecklenbrauker et al. (2011) and Molisch et al. (2009). The results of this paper can be used as preliminary steps toward addressing string stability issues in future work.

1.2. Related work and contributions

Research topics on event-based communication and control have attracted a great deal of attention in both control and communication communities (Hetel et al., 2017). It is beyond the scope of this paper to do an exhaustive literature review on this popular topic. Instead, this section will focus on discussing the relationship and connection between our proposed work and the existing research work on event/self triggered schemes under unreliable communication. For those who are interested in a complete review on self-triggered/event-triggered estimation and control, please see Heemels et al. (2012) for more details.

The issues of stability and performance under event-based strategies must be carefully examined in the presence of unreliable wireless communication. Prior work in Lehmann and Lunze (2012), Wu et al. (2014) and Zhang et al. (2001) has shown that the temporal communication failures caused by packet loss or delay may lead to stability issues for networked control systems. To address communication issues in networked control systems with event-based strategies, a great deal of research work (Dolk et al., 2017a; Dolk & Heemels, 2017; Guinaldo et al., 2012; Peng & Yang, 2013; Wang & Lemmon, 2009, 2011b; Yu & Antsaklis, 2013) have been proposed to find sufficient conditions on the maximum allowable number of successive packet drops (MANSD) or maximum allowable delay, under which the system stability and performance criteria, such as $\mathcal{H}_\infty$ (Peng & Yang, 2013) and $\mathcal{L}_p$ (Dolk et al., 2017a; Wang & Lemmon, 2009; Yu & Antsaklis, 2013), can be preserved under event/self-triggered strategies.

Two key assumptions for these prior results include that (1) wireless communication channels must be sufficiently reliable to strictly satisfy the MANSD or maximum allowable delay, and (2) variations on wireless channels must be decoupled from dynamics of the vehicle systems. These assumptions, however, may not hold for VNS because the *state-dependent* fading channels in VNS may lead to a burst of packet losses with non-zero probabilities, and are also highly dependent on the vehicle states, such as inter-vehicle distance, velocities and heading angles (Akki, 1994; Cheng et al., 2007). Such a correlation between vehicle and channel states clearly invalidates the use of separation principle in event-triggered design, which is widely adopted in existing literature (Borgers & Heemels, 2014; Li et al., 2016).

Another challenge of using event-based strategies under unreliable wireless communication is that a strictly positive *minimum inter-event time* (MIET) may not be guaranteed if packet loss or delay is present. As discussed in Mazo and Tabuada (2008), violation of MIET leads to Zeno phenomenon that generates infinite transmissions or samplings within a finite time interval and seriously hinders practical implementation of event-based strategies. One approach to address the potential Zeno issues is to combine time-triggered and event-triggered strategies such that the event-triggered scheme is designed based on a predefined equidistant time instances (e.g., periodic event-triggered scheme proposed in Abdelrahim et al., 2016a, 2016b; Dolk et al., 2017a; Heemels et al., 2013; Peng & Yang, 2013; Tallapragada & Chopra, 2012) and switched to a time-triggered scheme if packet loss or delay occurs (Dolk et al., 2017b; Guinaldo et al., 2012; Lehmann & Lunze, 2012). Although the MIET can be always guaranteed to be positive under the combined framework of event-triggered and time-triggered schemes, it is unclear, however, how efficient and effective such combined approaches may be in deep fading channels where a long string of consecutive packet loss may occur.

Motivated by the challenges discussed above, the objective of this paper is to design a new self-triggered communication scheme that ensures both stability of VNS and efficient use of communication resources by taking into account the state-dependent and burstiness properties of wireless channels in VNS. The key difference between the proposed self-triggered scheme in this paper and the others in the literature, such as Anderson et al. (2015), Gommans et al. (2014), Wang and Lemmon (2009) lies in two aspects. First, by adopting a state-dependent bursty fading channel model proposed in Hu and Lemmon (2013) and Hu and Lemmon (2015), this paper explicitly incorporates the knowledge of correlations between communication channel and vehicle states into the design process, which allows the self-triggered scheme to adaptively adjust the transmission frequency in response to any changes in channel conditions. This paper also shows that the inclusion of such correlation knowledge from the channel model is essential for the proposed self-triggered scheme to achieve efficient utilization of communication bandwidth. Second, unlike the combined framework that relies on a pre-selected minimum time interval to ensure a positive MIET, the proposed self-triggered scheme guarantees Zeno-free (finite number of transmissions or samplings over a finite time interval) transmission behavior in the presence of bursty-fading channels while still preserving specified system performance. In addition, this

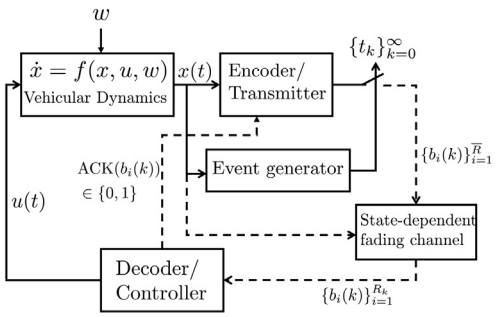

Fig. 1. Self-triggered vehicular networked system.

paper demonstrates communication efficiency of the proposed self-triggered scheme through extensive simulation results that compare communication performance under our proposed self-triggered scheme, such as minimum transmission time interval and average transmission time interval, against those under other existing event-based strategies (Li et al., 2017; Wang & Lemmon, 2011b).

The rest of this paper is organized as follows: Section 2 describes models of vehicle dynamics, wireless communication and control systems. Based on system models presented in Section 2, Section 3 provides formal definitions for stochastic hybrid system framework as well as stochastic stability. Section 4 discusses necessary assumptions needed to establish main results of this paper. With the assumptions stated in Section 4, Section 5 presents main results of this paper. The main results are applied to a leader–follower control example introduced in Section 2.5 and are verified through simulation results provided in Section 6. Section 7 concludes the paper.

Notations. Let $\mathbb{R}^n$ denote a n-dimensional Euclidean vector space, and $\mathbb{R}_+$, $\mathbb{Z}_+$ denote nonnegative reals and integers respectively. The infinity norm of a vector $x \in \mathbb{R}^n$ is denoted by $|x| := \max_{1\le i\le n} |x_i|$ where x_i is the *ith* element of the vector x. Consider a real valued function $x(\cdot) : \mathbb{R}_+ \to \mathbb{R}^n$, $x(t)$ denotes the value that function $x(\cdot)$ takes at time $t \in \mathbb{R}_+$. The left limit value of x at time t is denoted by $x(t^-)$. Given a time interval $[t_1, t_2)$ with $t_1 < t_2 \in \mathbb{R}_+$, the essential supremum of the function $x(t)$ over a time interval $[t_1, t_2)$ is denoted as $|x(t)|_{[t_1,t_2)} = \operatorname{esssup}_{t\in[t_1,t_2)} \|x(t)\|$ where $\|x(t)\|$ is the Euclidean norm of function x at time t. The function $x(t)$ is essentially bounded if there exists a positive real $M < \infty$ such that $|x(t)|_{\mathcal{L}_\infty} = \operatorname{esssup}_{t>0} \|x(t)\| \le M$.

A function $\alpha(\cdot) : \mathbb{R}_+ \to \mathbb{R}_+$ is a class $\mathcal{K}$ function if it is continuous and strictly increasing, and $\alpha(0) = 0$. $\alpha(t)$ is a class $\mathcal{K}_\infty$ function if it is class $\mathcal{K}$ and radially unbounded. A function $\beta(\cdot,\cdot) : \mathbb{R}_+ \times \mathbb{R}_+ \to \mathbb{R}_+$ is a class $\mathcal{KL}$ function if $\beta(\cdot, t)$ is a class $\mathcal{K}_\infty$ function for each fixed $t \in \mathbb{R}_+$ and $\beta(s,t) \to 0$ for each $s \in \mathbb{R}_+$ as $t \to +\infty$. $\beta(\cdot,\cdot)$ is an exp-$\mathcal{KL}$ function if there exist positive reals $c_i \in \mathbb{R}_+$, $i = 1, 2$ such that $\beta(s,t) = c_1 \exp(-c_2 t)s$.

2. System description

Fig. 1 shows a self-triggered control framework for a vehicular networked system that consists of blocks of *Vehicular Dynamics*, *Encoder/Transmitter*, *Event generator*, *State-dependent fading channel* and *Decoder/Controller*. The following subsections focus on the detailed descriptions of these blocks.

2.1. Vehicular dynamics

Consider that the dynamics of a vehicular system satisfy the following nonlinear ODE,

$$\dot{x} = f(x,u,w), \quad x(0) = x_0 \tag{1}$$

where $x \in \mathbb{R}^n$ is the system state that may represent inter-vehicle distance and relative bearing angles (see Section 2.5 in this paper or Hu & Lemmon, 2014), $u \in \mathbb{R}^m$ is control input and $w \in \mathbb{R}^\ell$ denotes external disturbance that is essentially ultimately bounded, i.e. $\exists W > 0$, s.t. $|w|_{\mathcal{L}_\infty} \le W$. The vector field $f(\cdot,\cdot,\cdot) : \mathbb{R}^n \times \mathbb{R}^m \times \mathbb{R}^\ell \to \mathbb{R}^n$ is a locally Lipschitz function.

The control objective for VNS is to track predefined set-points in the presence of bursty fading channels. The tracking performance is investigated under two communication constraints: (1) State measurements $x(t)$ are taken and only available to controller at discrete time instants $t_k \in \mathbb{R}_{\ge 0}$, $k \in \mathbb{Z}_{\ge 0}$; (2) The sampled state measurements $x(t_k)$ used for tracking control, are encoded by a finite number of symbols and are transmitted over a fading channel with time varying data rates.

2.2. Event-based communication: Encoder/transmitter and event generator

The continuous vehicular state $x(t)$ in Fig. 1 is sampled at discrete time instants $\{t_k\}_{k=0}^{\infty}$ with $t_k < t_{k+1}$ and $t_k \in \mathbb{R}_+, \forall k \in \mathbb{Z}_+$. Such strictly increasing time instants $\{t_k\}_{k=0}^{\infty}$ are generated by an *Event generator*, which decides when to transmit state information. The sampled state $x(t_k)$ at time instant t_k is quantized by an *Encoder* with a fixed number of $\bar{R}$ blocks of bits $\{b_i(k)\}_{i=1}^{\bar{R}}$. Each block consists of n binary bits and is used to encode the state information of vehicle. Thus, the continuous vehicular state at each *discrete* time instant t_k will be encoded and represented by one of the $2^{n\bar{R}}$ finite symbols. We assume that the symbol with $\bar{R}$ blocks of bits is assembled into $\bar{R}$ number of small packets with a packet length n, and sequentially transmitted across a wireless fading channel. In this paper, we assume that the time spent on quantization and packet-assembly is sufficiently small and its impact on system stability and performance can be safely neglected.[1]

Sequential Transmission in VNS. Unlike most stationary or slow varying wireless network, wireless channels in VNS often exhibit much faster variations due to high motions in vehicular transceivers (Cheng et al., 2007). Recent work has shown that vehicular wireless channels, such as V2V communication (Papadimitratos et al., 2009), are subject to small coherence time, which makes the transmission of a large size of packets fairly challenging. Motivated by this challenge, a sequential communication scheme is adopted in this paper to sequentially transmit prioritized small packets over wireless channels (Hu & Lemmon, 2015; Papadimitratos et al., 2009). Specifically, the sequential transmission scheme ensures that packets with the highest priority (most significant bits) are received first (Martins et al., 2006). In comparison to the conventional transmission policy that wraps all information into one single big packet, the sequential transmission protocol with small prioritized packets is able to recover the transmitted information with a reasonable accuracy in the presence of bursty fading channels.

[1] The time spent on quantization and packet-assembly is often related to packet processing time. It is well studied that the packet processing time is often of the order of microseconds or less (Kurose, 2005), and is thus negligible compared to the transmission time interval considered in this paper.

2.3. State-dependent V2V fading channel

The number of successfully received packets R_k at each transmission time instant t_k randomly changes due to channel fading. This paper adopts a state-dependent exponential bounded burstiness (SD-EBB) model to characterize stochastic variations on R_k (Hu & Lemmon, 2013). As shown by our recent work (Hu & Lemmon, 2015), the SD-EBB model was able to describe a wide range of fading channels including i.i.d. and Markov chain channels. More importantly, the SD-EBB model explicitly characterizes the probability bound on channel burstiness and its dependency on vehicle states, which has been proven to be essential for system stability (Hu & Lemmon, 2013, 2015). To be specific, let $h(\cdot)$ and $\gamma(\cdot)$ denote continuous, nonnegative, monotone decreasing functions from $\mathbb{R}_+$ to $\mathbb{R}_+$. Assume that the probability of successfully receiving R_k packets at time instant t_k satisfies

$$\Pr\{R_k \leq h(|x(t_k)|) - \sigma\} \leq e^{-\gamma(|x(t_k)|)\sigma} \tag{2}$$

with $\sigma \in [0, h(|x(t_k)|)]$. The function $h(|x(t_k)|)$ in SD-EBB model is a state-dependent threshold that separates the low bit-rate region from the high bit rate region in the channel state space. It monotonically decreases as vehicle states (e.g. inter-vehicle separation and relative bearing angle) deviates from the origin. The state-dependent function $h(|x(t_k)|)$ models the impact of large scale fading caused by path loss and directional antenna gain on data rates (Choudhury et al., 2002; Tse & Viswanath, 2005). The variable $\sigma \in [0, h(|x(t_k)|)]$ is the *dropout burst length* in the low bit-rate region. Thus, the left hand side of the SD-EBB model characterizes the probability of fading channels exhibiting a bursty packet loss with a burst length σ. The right-hand side of the SB-EBB model shows that such a bursty probability is exponentially bounded. The function $\gamma(|x(t_k)|)$ is a state-dependent exponent in the probability bound that characterizes how fast the probability of a bursty dropout decays as a function of dropout burst length within the low bit rate region.

The SD-EBB model can be used in a variety of vehicular applications, such as leader–follower formation control for ground transportation system (Cheng et al., 2007), air transportation systems (Park et al., 2014) and autonomous underwater vehicles (Akyildiz et al., 2005), where large inter-vehicle distance and vehicular velocities cause low data rate and more likely lead to deep fades, or in ad hoc wireless networks with directional antennae where changes in relative bearing angles between the transmitter and receiver may cause a deep fade. Example 1 shows how the SD-EBB model is obtained and related to the notion of *outage probability* which is well-known performance metric for fading channels.

Example 1. Let $X_i(k) \in \{0, 1\}$ denote a binary random variable at time instant t_k, with $X_i(k) = 1$ representing the successful reception of the ith block of bits (packet) and $X_i(k) = 0$ otherwise, then $R_k = \sum_{i=1}^{\bar{R}} X_i(k)$. For a given transmission power p and threshold γ_0, one has

$$\begin{aligned}\Pr\{X_i(k) = 1\} &= 1 - \Pr\{\text{SNR} \leq \gamma_0\} \\ &= 1 - \Pr\{pg^2/(\vartheta(x(t_k))N_0) \leq \gamma_0\} \\ &\triangleq \varpi(x(t_k)),\end{aligned} \tag{3}$$

where N_0 is the noise power, g is a random variable that characterizes the small scale fading, and $\vartheta(x(t_k))$ is a continuous, positive and monotonically increasing function that characterizes path loss and directional antenna gain in wireless channels, e.g., $\vartheta(x) = \cos\alpha/L^\nu$ with path loss exponent $\nu \in [2, 4]$ and vehicle state $x = [L; \alpha]$ where L is the distance between transmitter and receiver, and α is the bearing angle of directional antenna (Balanis, 2016; Stüber, 2011). $\varpi(|x(t_k)|)$ is the successful reception probability for the ith block of bits (packet) whose value increases as the vehicle state x moves toward the origin. With the probability in (3), one can obtain the SD-EBB characterization in (2) by using the Chernoff inequality (Hu & Lemmon, 2015). The selection of the functions $h(\cdot)$ and $\gamma(\cdot)$ depends on fading characteristics. Take the i.i.d. fading channel as an example with the state $x = [L; \alpha]$ (L is the inter-vehicle distance and α is a bearing angle of the directional antenna), suppose that the channel gain follows a Raleigh distribution (Goldsmith & Chua, 1997), then the functions take the form of $h(x) = c_1 e^{-c_2 \frac{L}{\cos\alpha}}$ and $\gamma(x) = c$ where the coefficients $c_1, c_2, c > 0$ are constant communication system parameters. Our prior results (please see Proof of Lemma III.3 in Hu and Lemmon (2015) for more details) also show how to select the function forms of $h(\cdot)$ and $\gamma(\cdot)$ for the case of Markov fading channels.

2.4. Remote tracking control system under event-based dynamic quantization

The control objective for VNS is to track predefined set-points. Let $x^d \in \mathbb{R}^n$ denote a desired constant set-point that is known to both encoder and decoder ahead of time. Let $\hat{x}$ denote an estimate of the vehicle state and $\hat{\tilde{x}} \triangleq \hat{x} - x^d$ represent an estimate of the tracking state. In between the transmission time instants t_k, $k \in \mathbb{Z}_{\geq 0}$, the state estimate $\hat{\tilde{x}}$ and control action $u(t)$ are generated as follows,

$$\begin{aligned}&\dot{\hat{\tilde{x}}} = f(\hat{\tilde{x}} + x^d, \kappa(\hat{\tilde{x}}), 0) \\ &u = \kappa(\hat{\tilde{x}}), \quad \forall t \in [t_k, t_{k+1})\end{aligned} \tag{4}$$

where $\kappa(\cdot) : \mathbb{R}^n \to \mathbb{R}^m$ is a nominal feedback control law ensuring that the state estimate $\hat{\tilde{x}}$ in the tracking control system (4) asymptotically converges to zero. At each transmission time instant t_k, the state estimate $\hat{\tilde{x}}(t_k^+)$ is reset to be a new value obtained from a *dynamic quantizer*. The dynamic quantizer,[2] in the *Encoder/Decoder* block is defined by three parameters, $R_k \in \mathbb{Z}_{\geq 0}$ (a random variable that defines the number of blocks of bits received at time instant t_k), $\hat{\tilde{x}}(t_k)$ (state estimate at time instant t_k) and $U(t_k)$ (an auxiliary variable that defines the size of quantization regions at time instant t_k). Consider a box dynamic quantizer and let $\bar{\tilde{x}}(t_k)$ denote the center of a hypercubic box with an edge length $2U(t_k)$, the quantizer divides the hypercubic box into 2^{nR_k} equal smaller sub-boxes after receiving R_k number of blocks of bits. The sub-box that contains the true value of vehicle state $\bar{x}(t_k)$ is encoded by $\{b_i(k)\}_{i=0}^{R_k}$. Let $\mathcal{R}_k$ denote a set of symbols that are represented by the R_k number of binary bits, $\{b_i(k)\}_{i=0}^{R_k}$ and $g_{\bar{x}} : \mathbb{R}_+ \times \mathcal{R}_k \times \mathbb{R}^n \times \mathbb{R}_+ \to \mathbb{R}^n$ denote a function that updates the state estimate after receiving a symbol $\{b_i(k)\}_{i=0}^{R_k}$. Let $T_k \triangleq t_k - t_{k-1}$ denote a time interval for the kth transmission and let $g_U : \mathbb{R}_+ \times \mathbb{R}^n \times \mathbb{R}_+ \to \mathbb{R}_+$ denote a function that updates the size of quantization regions. Note that functions $g_{\bar{x}}, g_U$ and time intervals $\{T_k\}_{k\in\mathbb{Z}_+}$ are parameters that need to be designed to assure system stability. The methods to design these parameters are discussed in Section 5. Thus, the new state estimate $\hat{\tilde{x}}(t_k^+)$ after receiving a symbol $\{b_i(k)\}_{i=0}^{R_k}$ can be updated according to the following equations

$$\hat{\tilde{x}}(t_k^+) = g_{\bar{x}}\left(T_k, \{b_i(k)\}_{i=0}^{R_k}, \hat{\tilde{x}}(t_k), U(t_k)\right), \tag{5}$$

$$U(t_k^+) = U(t_k)2^{-R_k} \tag{6}$$

[2] As discussed in prior work (Tatikonda & Mitter, 2004; Wong & Brockett, 1999) the use of dynamic quantization assures that the system state can be accurately observed asymptotically. Such asymptotic performance plays an important role of achieving *almost sure asymptotic stability* under fading channels.

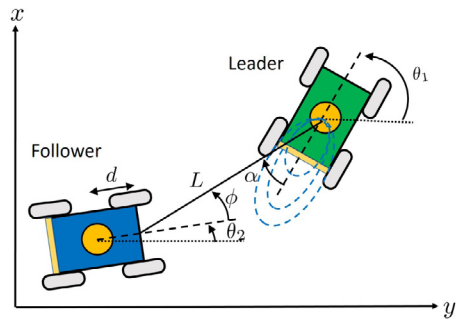

Fig. 2. Leader–follower formation control.

with $\hat{\bar{x}}(t_k^+)$ being the center of a new hypercubic box with an updated edge length $2U(t_k^+)$. Let $T_k \triangleq t_k - t_{k-1}$ denote a time interval for the kth transmission. Until the $(k+1)$th transmission, i.e., time instant t_{k+1}, the size of a quantization region $U(t_{k+1})$ is propagated according to

$$U(t_{k+1}) = g_U(T_{k+1}, \hat{\bar{x}}(t_k^+), U(t_k^+)). \tag{7}$$

and then the procedure of (5)–(7) is repeated.

Since both encoder and decoder use Eqs. (5)–(7) to update the pair $\{\hat{\bar{x}}(t_k^+), U(t_k^+)\}$ in the dynamic quantizer, it is important to ensure that the encoder and decoder are synchronized with the number of bits that are successfully received. To achieve that, this paper assumes that there exists a noiseless feedback channel that reliably delivers acknowledge signals from decoder to encoder to indicate a successful reception of a block of bits.

2.5. Leader–follower formation control

The system model considered in Eq. (1) can be illustrated via a leader–follower control example shown in Fig. 2. The leader–follower example will also be used as a simulation example in Section 6. The kinematic model for both vehicles in the leader–follower example is provided as follows:

$$\dot{p}_{x,i} = v_i \cos\theta_i, \quad \dot{p}_{y,i} = v_i \sin\theta_i, \quad \dot{\theta}_i = \omega_i. \tag{8}$$

where $p_{x,i}, p_{y,i}, i = 1, 2$ are the horizontal and vertical positions of leader ($i = 1$) and follower ($i = 2$), respectively, and $\theta_i, i = 1, 2$ are orientations of leader and follower relative to the horizon. Based on the kinematic model in (8), the leader–follower system in Fig. 2 satisfies the following ODE (Hu & Lemmon, 2015),

$$\begin{aligned} \dot{L} &= v_1 \cos\alpha - v_2 \cos\phi - d\omega_2 \sin\phi \\ \dot{\alpha} &= \tfrac{1}{L}(-v_1 \sin\alpha - v_2 \sin\phi + d\omega_2 \cos\phi) + \omega_1 \end{aligned} \tag{9}$$

where d is the length from the center of vehicle to its front. v_1 and ω_1 are leader's speed and angular velocity, while v_2 and ω_2 are follower's speed and angular velocity. L is the inter-vehicle distance that is measurable by both leader and follower, α and ϕ are relative bearing angles of leader to follower and follower to leader respectively. It is assumed that α is only measurable to the leader, and ϕ is available for the follower. What is not directly known to the follower is the bearing angle α. Therefore, the leader–follower pair characterizes a vehicular networked system that requires the leader to transmit its bearing angle α to the follower over a wireless communication channel. The wireless channel is accessed by a directional antenna that is mounted at the back of the leader where the channel exhibits exponential burstiness and satisfies the state dependent EBB characterization in (2) with (L, α) as the vehicle state x. As shown in Fig. 2, the directional antenna has a radiation range from $-\frac{\pi}{2} \le \alpha \le \frac{\pi}{2}$ out of which the communication channel is assumed to be zero.

With limited information on α, the control objective is to have the follower adjust its speed v_2 and angular velocity ω_2 to achieve desired inter-vehicle separation L_d and bearing angle α_d almost surely in the presence of deep fades. A standard input to state feedback linearization method is used to generate control inputs (v_2, ω_2) over each transmission time interval $[t_k, t_{k+1})$,

$$\begin{bmatrix} v_2 \\ \omega_2 \end{bmatrix} = \begin{bmatrix} -\cos\phi & -L\sin\phi \\ -\frac{\sin\phi}{d} & \frac{L}{d}\cos\phi \end{bmatrix} \left(\begin{bmatrix} K_L(L_d - L) \\ K_\alpha(\alpha_d - \hat{\alpha}) \end{bmatrix} - \begin{bmatrix} \cos\hat{\alpha} & 0 \\ -\frac{\sin\hat{\alpha}}{L} & 1 \end{bmatrix} \begin{bmatrix} v_1 \\ \omega_1 \end{bmatrix} \right) \tag{10}$$

where (K_L, K_α) are the controller gains. $\hat{\alpha}$ represents the prediction of bearing angle over $[t_k, t_{k+1})$ that satisfies

$$\dot{\hat{\alpha}} = K_\alpha(\alpha_d - \hat{\alpha}), \hat{\alpha}(t_k) = \alpha^q(t_k) \tag{11}$$

with the bearing angle estimate $\alpha^q(t_k)$ as an initial value.

Let $g_v : \mathbb{R}_+ \to \mathbb{R}_+$ and $g_\omega : \mathbb{R} \to \mathbb{R}$ denote functions that characterize how the leader changes its speed and angular velocity respectively, in response to inter-vehicle distance L and relative bearing angle α. The real values of speed v_1 and angular velocity ω_1 can then be modeled by adding essentially bounded noise. Mathematically, one has $v_1 = g_v(L) + n_1$ and $\omega_1 = g_\omega(\alpha) + n_2$ with $|n_i|_\infty \le M, i = 1, 2$. With the controller in (10) and (11), the closed-loop dynamics of inter-vehicle distance L and bearing angle α therefore satisfy following differential equations over time interval $[t_k, t_{k+1})$.

$$\begin{aligned} \dot{L} &= K_L(L_d - L) + (g_v(L) + n_1)(\cos\alpha - \cos\hat{\alpha}) \\ \dot{\alpha} &= \tfrac{(g_v(L)+w_1)}{L}(\sin\hat{\alpha} - \sin\alpha) + K_\alpha(\alpha_d - \hat{\alpha}) \\ &\quad + g_\omega(\alpha) + n_2 - g_\omega(\hat{\alpha}) \end{aligned} \tag{12}$$

for all $k \in \mathbb{Z}_+$. The dynamic model presented in (12) will be used to simulate leader–follower networked system in Section 6.

3. Problem formulation

Let $\bar{x}(t) = x(t) - x^d$ denote the tracking error and $e(t) \triangleq \bar{x}(t) - (\hat{x}(t) - x^d) = x(t) - \hat{x}(t)$ denote the estimation error induced by bursty fading channels. The closed-loop dynamics of VNS defined in (1), (2), (4) and (5)–(7) can be reformulated as below,

$$\dot{\bar{x}}(t) = f_{\bar{x}}(\bar{x}, e, w), \quad \forall t \in (t_k, t_{k+1}) \tag{13a}$$
$$\dot{e}(t) = f_e(\bar{x}, e, w), \quad \forall t \in (t_k, t_{k+1}) \tag{13b}$$
$$U(t_{k+1}) = f_U(T_{k+1}, R_k, \bar{x}(t_k), e(t_k^+), U(t_k)) \tag{13c}$$
$$e(t_k^+) = h_e(T_k, R_k, \bar{x}(t_k), e(t_k), U(t_k)) \tag{13d}$$
$$U(t_k^+) = h_U(R_k, U(t_k)) \tag{13e}$$

where

$$\begin{aligned} f_{\bar{x}}(\bar{x}, e, w) &\triangleq f(\bar{x} + x^d, \kappa(\bar{x} - e), w) \\ f_e(\bar{x}, e, w) &\triangleq f_{\bar{x}}(\bar{x}, e, w) - f(\bar{x} - e + x^d, \kappa(\bar{x} - e), 0) \\ f_U(T, R, \bar{x}, e^+, U) &\triangleq g_U(T, \bar{x} - e^+ + x^d, 2^{-R}U) \\ h_e(T, R, \bar{x}, e, U) &\triangleq \bar{x} - g_{\bar{x}}(T, R, \bar{x} - e + x^d, U) \\ h_U(R, U) &\triangleq 2^{-R}U. \end{aligned}$$

Eqs. (13a) and (13b) represent continuous dynamics of the closed-loop VNS, while Eq. (13c) characterizes a controlled stochastic process. Eqs. (13d) and (13e) represent the stochastic jumps for continuous and discrete states, respectively. The randomness of this stochastic hybrid systems comes from the stochastic process $\{R_k\}_{k=0}^\infty$ that is assumed to satisfy the SD-EBB model in (2).

Under the closed-loop VNS framework, the objective of this paper is to design an event based communication scheme to ensure *stochastic stability* for VNSs in (13). In particular, this paper considers both sample-based and mean stability. Sample-based stability emphasizes the behavior of almost all sample paths toward or around the origin while mean stability stresses system behavior in expectation. Besides stochastic stability, this paper also requires that the designed event-based communication scheme must ensure Zeno-free transmission. The formal definitions of Zeno-free transmissions and stochastic stability are provided as below,

Definition 2 (*Zeno-free Transmission*)**.** A transmission sequence $\mathcal{I} = \{t_k\}_{k=0}^{N}$ with $N \in \mathbb{Z}_+$ is said to be Zeno-free if $\forall 0 \leq k \leq N-1$, there always exists a $\tau > 0$ such that $t_{k+1} - t_k \geq \tau$.

Definition 3 (*Stochastic Stability Kozin, 1969*)**.** Consider a closed-loop VNS framework defined in (13), and let $\bar{x}_0 \triangleq x(0) - x^d \in \mathbb{R}^n$ denote the initial state,

E1 The system in (13) with $w = 0$ is *asymptotically stable in expectation* with respect to origin, if for any given $\epsilon > 0$, there exists $\delta(\epsilon)$ such that $|\bar{x}_0| \leq \delta$ implies

$$\mathbb{E}\{|\bar{x}(t)|\} < \epsilon \tag{14}$$

and $\lim_{t\to\infty} \mathbb{E}\{|\bar{x}(t)|\} = 0$.

E2 The system in (13) with $|w|_{\mathcal{L}_\infty} \leq M$ is *uniformly asymptotically bounded in expectation*, if for a given $(\Delta(M), \Delta_0(M))$ with $\Delta_0, \Delta > 0$, there exists a $\epsilon(M, \Delta_0) > 0$ such that for $|\bar{x}(0)| \leq \Delta_0$,

$$\mathbb{E}\{|\bar{x}(t)|\} \leq \epsilon(M, \Delta_0) \quad \forall t \in \mathbb{R}_{\geq 0} \tag{15}$$

and $\lim_{t\to\infty} \mathbb{E}\{|\bar{x}(t)|\} \leq \Delta(M)$.

P1 The system in (13) with $w = 0$ is *almost surely asymptotically stable* with respect to origin, if for any given $\epsilon, \epsilon' > 0$, there exists $\delta(\epsilon, \epsilon')$ such that $|\bar{x}_0| \leq \delta$ implies

$$\Pr\{\sup_{t\geq 0} |\bar{x}(t)| \geq \epsilon'\} < \epsilon \tag{16}$$

and $\Pr\{\lim_{\tau\to\infty} \sup_{t\geq\tau} |\bar{x}(t)| \geq \epsilon'\} = 0$.

P2 The system in (13) with $|w|_{\mathcal{L}_\infty} \leq M$ is *practically stable in probability* if for a given $(\Delta(M), \Delta_0(M))$ with $0 < \Delta_0 < \Delta$ and for any $\epsilon' > 0$, there exists a $\epsilon(M, \Delta) > 0$ such that for $|\bar{x}(0)| \leq \Delta_0$,

$$\lim_{t\to+\infty} \Pr\{|\bar{x}(t)| \geq \Delta + \epsilon'\} \leq \epsilon(M, \Delta). \tag{17}$$

Remark 1. Among all four definitions of stochastic stability, *almost sure asymptotic stability* is the strongest one that requires almost all samples of the system trajectories defined in (13) asymptotically converge to origin with probability one. The notion of *mean stability* (**E1**) is weaker because it only requires that the expected value of system trajectory's magnitude asymptotically goes to zero. In general, *mean stability* does not imply *almost sure asymptotic stability* while the latter implies the former. For more discussions on stochastic stability, please refer to Kozin (1969).

Remark 2. If a non-vanishing but bounded external disturbance is present in VNS, asymptotic stability (i.e., **E1** and **P1**) cannot be guaranteed. The notion of practical stability defined in **E2** and **P2** is therefore introduced to characterize system behavior around a compact set in expectation or in probability. Specifically, *uniformly asymptotic boundedness in expectation* (**E2**) requires that the expectation of a norm of system states is uniformly bounded and asymptotically converges to a constant that depends on the magnitude of external disturbance. The notion of *practical stability in probability* requires that the probability (**P2**) of system trajectories leaving a compact set is bounded from above by a function that depends on both the magnitude of external disturbance and the size of compact set. By Markov's Inequality, it is straightforward to show that **E2** implies **P2**.

With VNS system framework and notions of stochastic stability defined, the problem of this paper is formally stated as below

Problem 4. Consider a closed-loop VNS formulated in (13), the problem is to design functions $g_{\bar{x}}$ and g_U, and determine the transmission time intervals $\{T_k\}_{k\in\mathbb{Z}_+}$ under which the VNS satisfies the stochastic stability notions defined in Definition 3.

4. Assumptions

This section presents two main assumptions that are needed to establish our main results.

Assumption 5. Consider a closed-loop VNS defined in (13), the subsystem $\bar{x}$ defined in (13a) is *input-to-state stable* (ISS) from $\bar{x}$ to estimation error e and external disturbance w. In particular, assume that there exist a concave class $\mathcal{KL}$ function $\beta(\cdot,\cdot)$, a class $\mathcal{K}$ function $\chi_2(\cdot)$ and a positive constant $\overline{\chi}_1 > 0$ such that

$$|\bar{x}(t)| \leq \beta(|\bar{x}(t_0)|, t - t_0) + \overline{\chi}_1(|e|_{[t_0,t]}) + \chi_2(|w|_{[t_0,t]}) \tag{18}$$

The subsystem $\bar{x}$ is *exponentially input-to-state stable* (Exp-ISS) if $\beta(\cdot,\cdot)$ is an exp-$\mathcal{KL}$ and $\chi_2(\cdot)$ is a linear function.

Remark 3. The ISS assumption is used to ensure *stability in expectation* (**E1** and **E2** in Definition 3) while the assumption of exp-ISS is needed for almost sure asymptotic stability (**P1** in Definition 3) .

Assumption 6. Suppose there exist $0 < w_1 < w_2, L_x, L_e, L_w \in \mathbb{R}_+$ and a nonnegative definite function $W(e)$ such that the subsystem e in Eq. (13b) satisfies

$$w_1|e| \leq W(e) \leq w_2|e| \tag{19a}$$

$$\nabla W(e) f_e(\bar{x}, e, w) \leq L_e W(e) + L_x|\bar{x}| + L_w|w| \tag{19b}$$

Remark 4. Assumption 6 is equivalent to the Exp-ISS assumption for subsystem e with respect to x and w (Nešić & Teel, 2004). This assumption is weaker than the uniformly Lipschitz assumption stated in Hu and Lemmon (2014) since the latter is a special case ($L_x = 0$) of the former. To see this, the uniformly Lipschitz assumption suggests that there exists a $L_f > 0$ such that $|f(x,u,w) - f(\hat{x},u,0)| \leq L_f(|x-\hat{x}| + |w|), \forall x, \hat{x} \in \Omega_x$ where Ω_x is a compact set. This uniformly Lipschitz assumption on the vector field f implies that $\frac{d|e|}{dt} \leq L_f|e| + L_f|w|$ which is a special case of (19b) with $L_x = 0$.

5. Main results

This section presents the development of a self-triggered communication scheme to ensure *stochastic stability* for VNS defined in (13). In particular, the proposed self-triggered transmission scheme generates a (sporadic) transmission sequence $\{t_k\}_{k=0}^{\infty}$ under which the VNS in (13) is either *asymptotically stable in expectation* (Theorem 8) or *almost surely asymptotically stable* (Theorem 9) without external disturbances ($w = 0$), and either *uniformly asymptotically bounded in expectation* (Theorem 10) or

practically stable in probability (Theorem 11) with bounded external disturbances. Under the self-triggered transmission scheme, the second main result (Proposition 12) of this paper is to construct a feasible event-based encoder/decoder pair (i.e., function g_x in (5) and g_U in (7)) in which the event-based dynamic quantizer does not saturate at any transmission time instant, that is, system states in (13) are guaranteed to be captured by the proposed event-based encoder/decoder.

The following technical lemma is needed to prove the main results by showing that the expectation of quantization resolution $\mathbb{E}(2^{-R_k})$ can be bounded by a function of the system state under a state-dependent bursty fading channel.

Lemma 7 (*Hu & Lemmon, 2014*)**.** *Consider a SD-EBB channel model in (2), define a function* $G(s) = e^{-h(s)\gamma(s)}(1+h(s)\gamma(s))$, $s \in \mathbb{R}_+$, *then*

$$\mathbb{E}(2^{-R_{k+1}}) \leq G(|x(k+1)|) \tag{20}$$

and $G(s) \in [0,1], \forall s \in \mathbb{R}_+$ *is a strictly increasing function with* $G(s) \to 0 \iff h(s)\gamma(s) \to +\infty$ *and* $G(s) \to 1 \iff h(s)\gamma(s) \to 0$.

Proof. The proof is omitted due to the space limitation. Please refer to Hu and Lemmon (2014) for the details of the proof.

Remark 5. The function $G(\cdot)$ is directly related to functions $h(\cdot)$ and $\gamma(\cdot)$ in the SD-EBB model and can therefore be viewed as a priori knowledge of the state-dependent fading channel.

Inequality (20) implies that quantization error decreases as the system state x approaches its origin. It is easy to see that $G(|x|) \to 1$ as $h(|x|) \to 0$, which corresponds to the scenario where vehicles are far apart and beyond communication range. This paper will focus on the situation when vehicles are within communication range and the SD-EBB model provides a reasonable bound on channel conditions. In particular, let $\Omega_x = \{x \in \mathbb{R}^n \big| |x| < G^{-1}(w_1/w_2)\}$ with $w_2 > w_1 > 0$ defined in Assumption 6, denote the region that communications between vehicles are available. Since $G(\cdot) \in [0,1]$ is a continuous and strictly monotonically increasing function, the inverse of $G(\cdot)$ exists and is also continuous, strictly monotonically increasing. Thus, Ω_x is a nonempty and open set and $G(|x|) < 1, \forall x \in \Omega_x$. The stability results in Section 5.1 will be examined under the situation that vehicles are within the communication range, i.e., $x \in \Omega_x$.

5.1. Self-triggering to achieve stochastic stability

A self-triggered scheme is developed in this section to ensure stochastic stability defined in Definition 3. With Assumptions 5 and 6, this section first presents two theorems showing that the VNS defined in (13) can asymptotically track pre-defined set-points in expectation (Theorem 8) under the ISS assumption or almost surely (Theorem 9) under the exp-ISS assumption without external disturbances, i.e., $w = 0$.

Theorem 8. *Consider a closed-loop VNS in (13) without external disturbance* ($w = 0$) *and a SD-EBB channel model in (2), suppose the ISS assumptions in Assumptions 5 and 6 hold, the system is asymptotically stable in expectation with respect to the origin, if the transmission time instants* $\{t_k\}$ *are generated by*

$$t_{k+1} = t_k + \frac{1}{L_e}\ln\Big(1 + \frac{1 - \frac{w_2}{w_1}G(|x(t_k)|)}{\frac{w_2}{w_1}G(|x(t_k)|) + \frac{L_x\bar{x}_1}{L_e w_1}}\Big). \tag{21}$$

within the communication range, i.e., $x \in \Omega_x$. *FurthermoreFurthermore, if the vehicle system is within the communication range, i.e.,* $x \in \Omega_x$, *there exists* $\underline{\Delta} > 0$ *such that the transmission time interval* $t_{k+1} - t_k \geq \underline{\Delta}, \forall k \in \mathbb{Z}_+$, *i.e. the self triggered scheme in (21) assures Zeno-free behavior.*

Proof. See the Appendix.

Remark 6. The transmission time intervals $\{T_k\}_{k=0}^{\infty}$ with $T_k = t_{k+1} - t_k$ generated by (21) monotonically increase when system states, such as inter-vehicle distance and bearing angles, move toward the origin. This property implies that VNS under the proposed self-triggered scheme can transmit less frequently when a good channel condition is guaranteed by either reducing inter-vehicle distance or aligning directional antennae mounted in both vehicles. The function G in (21) defined in Lemma 7 quantitatively assesses and predicts how channel conditions vary as a function of system states. Such quantitative predictions on channel conditions are used in the design of a self triggered communication scheme to ensure an efficient utilization of channel bandwidth by adaptively adjusting its transmission frequency.

Theorem 9. *Suppose all conditions and assumptions in Theorem 8 hold, and the subsystem* $\bar{x}$ *is Exp-ISS (i.e., Exp-ISS in Assumption 5) holds, the VNS in (13) without external disturbance is* almost surely asymptotically stable *with respect to origin if the transmission time sequence is recursively generated by (21). The non-Zeno transmission is guaranteed if vehicles are within the communication range (i.e.,* $x \in \Omega_x$*).*

Proof. The proof is provided in the Appendix.

Since the strong notion of *asymptotic stability* cannot be guaranteed in the presence of non-vanishing disturbance, this section shows that weak notions of *uniformly asymptotic boundedness in expectation* (**E2**) and *practical stability in probability* (**P2**) can be achieved under the self triggered scheme defined in (21).

Theorem 10. *Consider the VNS defined in (13) with essentially bounded external disturbance* $|w|_{\mathcal{L}_\infty} \leq M$, *and suppose the fading channel satisfies the SD-EBB characterization defined in (2). Suppose the ISS assumption in Assumptions 5 and 6 holds, if the transmission time sequence* $\{t_k\}$ *is generated by (21), then the system in (13) is uniformly asymptotically bounded in expectation (**E2**).*

Proof. See the Appendix.

Theorem 11. *Suppose the hypothesis in Theorem 10 holds, then the system in (13) is practically stable in probability (**P2**). More specifically, there exists a class* $\mathcal{KL}$ *function* $\beta_\epsilon(\cdot,\cdot)$ *such that*

$$\lim_{t\to+\infty} \Pr\{|\bar{x}(t)| \geq \Delta + \epsilon\} \leq \beta_\epsilon(M, \Delta). \tag{22}$$

Proof. See the Appendix.

Remark 7. The probability bound in (22) measures the safety level as a function of the size of a safe region Δ as well as the magnitude of external disturbance M. This safety metric provides a trade-off between the choices of Δ and M, which shows that the system is more likely to be safe with a smaller magnitude of external disturbance M and a larger safety region Δ.

5.2. Event-based encoder/decoder design

The stability results hold under the hypothesis that system states $\bar{x}(t_k)$ at each time instant $t_k, \forall k \in \mathbb{Z}_{\geq 0}$ must be captured by the encoder and decoder defined in (5)–(7) with parameters $(\hat{\bar{x}}(t_k^+), U(t_k^+))$ representing the centroid and size of dynamic quantizer respectively. This hypothesis is proved in the following proposition by showing that an *Encoder/Decoder* pair can be designed to recursively construct and synchronize the parameters $(\hat{\bar{x}}(t_k^+), U(t_k^+))$ as time increases. For notation simplicity, let $\hat{\bar{x}}_k^+ := \hat{\bar{x}}(t_{k^+})$ and $U_k^+ := U(t_k^+)$.

Proposition 12. *Suppose Assumptions 5 and 6 hold, and let* $\{t_k\}_{k=0}^{\infty}$ *denote a transmission time sequence generated by (21) and* $T_k = t_{k+1} - t_k$. *Suppose the initial value of the pair* $(\hat{\bar{x}}_0^+, U_0^+)$ *and the number of successfully received bits* $R_k, \forall k \in \mathbb{Z}_{\geq 0}$, *are known to the* Encoder *and* Decoder *by noiseless feedback channels, if the sequence of information pairs* $\{\hat{\bar{x}}_k^+, U_k^+\}_{k=1}^{\infty}$ *is constructed by*

$$U_{k+1}^+ = \frac{2^{-R_{k+1}}}{\eta_{k+1}} \left(\frac{v_2}{v_1} e^{L_e T_k} U_k^+ + \frac{e^{L_e T_k} - 1}{v_1 L_e} \left(L_x \beta(|\hat{\bar{x}}_k^+| + U_k^+, 0) + L_w M + L_x \chi_2(M) \right) \right), \tag{23a}$$

$$\hat{\bar{x}}_{k+1}^+ = U_{k+1}^+ 2^{R_{k+1}} \sum_{j=1}^{R_{k+1}} \frac{1}{2^j} q\big(b_j(k+1)\big) + \Phi(\hat{\bar{x}}_k^+, T_k), \tag{23b}$$

where $\eta_k = 1 - \frac{L_x \bar{\alpha}_1}{w_1 L_e}(e^{L_e T_k} - 1) > 0$, *and* $\Phi(s,t)$ *is the solution to the following differential equation*

$$\dot{\bar{x}} = f_{\bar{x}}(\bar{x}, 0, 0), \quad \bar{x}(0) = s. \tag{24}$$

where $f_{\bar{x}}(\cdot,\cdot,\cdot)$ *is defined in (13a) and* $q(\cdot) : \{0,1\}^n \to \{-1,1\}^n$ *is a function that maps the binary value of the bit vector to a n dimensional vector whose elements are* ± 1, *i.e.,*

$$q_i(b) = \begin{cases} 1 & \text{if the } i\text{th bit in bit-vector } b \text{ is } 1, \\ -1 & \text{otherwise}. \end{cases}$$

then the estimation error $e(k) = \bar{x}(t_k) - \hat{\bar{x}}_k^+$ *is bounded as*

$$|\bar{x}(t_k) - \hat{\bar{x}}_k^+| \leq U_k \tag{25}$$

for all $k \in \mathbb{Z}_{\geq 0}$.

Proof. See the Appendix.

Remark 8. $\eta_k > 0$ holds $\forall k \in \mathbb{Z}_+$ if the self-triggered scheme in (21) is adopted. The recursive functions in (23a) and (23b) correspond to the Encoder/Decoder structure defined in (5)–(7). The Encoder/Decoder design in (23a) and (23b) generalizes the result in Hu and Lemmon (2014). One can recover the Encoder/Decoder structure in Hu and Lemmon (2014) by setting $L_x = 0$. This generalization is possible due to Assumption 6 which is weaker than the uniformly Lipschitz assumption in Hu and Lemmon (2014).

Remark 9. Eq. (23b) is a recursive rule updating the centroid of a dynamical uniform quantizer (Martins et al., 2006). The structure of solution $\Phi(s,t)$ can be determined offline by solving the nonlinear differential equation (24) (nominal system without considering the network effect) with an initial value. In general, obtaining an analytic solution for a nonlinear ODE (24) is difficult, but one can obtain approximation on the solution by integrating the function $f_{\bar{x}}$ from t_k to $t_k + T_k$, i.e., $\Phi(\hat{\bar{x}}_k^+, T_k) = \hat{\bar{x}}(t_k + T_k) = \hat{\bar{x}}(t_k^+) + \int_{t_k}^{t_k+T_k} f_{\bar{x}}(\hat{\bar{x}}(t), 0, 0)dt$. However, the analytic solution can be obtained if the function $f_{\bar{x}}$ is linear, e.g., $f(\bar{x}, 0, 0) = A\bar{x}$, then one has $\Phi(\hat{\bar{x}}_k^+, T_k) = \exp(AT_k)\hat{\bar{x}}_k^+$.

6. Simulation results

This section presents simulation results examining advantages of the proposed self triggered scheme over traditional event triggered schemes in the leader–follower example. In the simulation, the mathematical model presented in (12) is used to simulate dynamics of the leader–follower system.

A two-state Markov chain model is used to simulate the fading channel between the leader and the follower. The two-state Markov chain model has one state representing the good channel state and the other representing the bad channel state. The good channel state means that a transmitted bit is successfully received, while the bad state means that a transmitted bit is lost. Following the two-state Markov chain model in Zhang and Kassam (1999), this simulation uses $p_{12} = 0.08\sqrt{\frac{\pi}{2}r}$ to represent the transition probability from a good state to a bad state, and $p_{21} = 0.08\sqrt{\frac{\pi}{2}}\frac{\sqrt{r}}{e^{0.25r}-1}$ to represent the transition probability from a bad state to a good state, where $r = \frac{L}{p\cos\alpha}$ and p is the transmission power. It is clear that the transition matrix for this two-state Markov chain model is a function of vehicular states (L and α) for a fixed transmission power p. Following the results in Hu and Lemmon (2015), the SD-EBB functions used in this simulation are $h(\alpha, L) = 0.8\bar{R}e^{-0.25\frac{L}{p\cos\alpha}}$ and $\gamma(\alpha, L) = 8\frac{p\cos\alpha}{L}$, with $\bar{R} = 4$ as the total number of bits transmitted over each time interval and $p = 8$ as the transmission power level. The initial inter-vehicle distance and bearing angle are $L(0) = 15\ m$ and $\alpha(0) = -30°$. The controller gains are $K_L = K_\alpha = 1$. Let the leader's speed v_1 and angular velocity ω_1 be $v_1 = 0.8L$ and $\omega_1 = 2.2\alpha$, respectively. The theoretical results are verified based on a Monte Carlo simulation method under which each simulation example is run 100 times over a time interval from 0 to 10 s.

The first simulation is to verify *almost surely asymptotic stability* of the leader–follower example under the proposed self-triggered scheme in (21) (Theorem 9). The upper plots in Fig. 3 show the maximum (red dashed-dot lines) and minimum (blue dashed lines) value of inter-vehicle distance L and bearing angle α over all the 100 samples from 0 to 10 s. From these plots, one can easily see that the maximum and minimum values of the system states asymptotically converge to desired set-points $L_d = 4\ (m)$ and $\alpha_d = 20°$ as time increases. This is the behavior that one would expect if a system is almost surely asymptotically stable. The lower plots in Fig. 3 show one sample of the inter-transmission time interval T_k (left plot) and the number of received bits R_k (right plot) that are used to achieve system performance shown in the upper plots. The transmission time interval T_k is generated by (21). It is clear from the plots that the self-triggered transmission policy starts with a small T_k when the leader–follower communication begins in a bad channel region due to a large inter-vehicle distance and bearing angle. As the leader–follower system gradually approaches its desired formation, the self-triggered communication scheme adaptively increases the inter-transmission time interval to ensure efficient use of communication bandwidth.

The second simulation is to compare performance of the proposed self-triggered scheme in (21) against conventional event-triggered scheme in Wang and Lemmon (2011a). For the purpose of comparison, a state dependent event-triggered scheme in Wang and Lemmon (2011a) was used to trigger the transmission whenever the estimation error exceeded a state dependent threshold. Let $|e(t)| = |\alpha(t) - \hat{\alpha}(t)| \leq 0.1591|[\alpha(t) - \alpha_d, L(t) - L_d]|$ be the triggering condition, and the threshold was selected to assure the same convergent performance as our self-triggered method but in the absence of channel fading.

Fig. 4 shows the comparison of both transmission time interval and tracking performance for the leader–follower example under proposed self-triggered scheme (marked by red squares) in (21) and event-triggered scheme (marked by blue diamonds) in Wang and Lemmon (2011a) over a wide range of formations, from $\alpha_d = 0°$ to $\alpha_d = 50°$. The tracking performance is compared by calculating the expected[3] average tracking error of inter-vehicle

[3] The expectation is approximated by the average of 100 sample runs, i.e., $\mathbb{E}\frac{1}{10}\int_0^{10}|x(t) - x^d|dt \approx \frac{1}{100}\sum_{i=1}^{100}\frac{1}{10}\int_0^{10}|x_i(t) - x^d|dt$ where $x = [L; \alpha]$ and x_i is the ith sample run.

distance and bearing angles over a time interval [0, 10]. The bottom plots of Fig. 4 show that both triggering schemes achieve quite similar tracking performance for inter-vehicle distance L and bearing angle α over all desired formations. The results in the top left plot of Fig. 4 show that the minimum transmission time interval T_{min} that is used to achieve the tracking performance under our proposed self-triggered scheme (around $T_{min} = 0.04$ s) is approximately 40 times larger than that generated by the event-triggered scheme ($T_{min} = 0.001$ s). Note that the minimum transmission time interval determines the channel bandwidth that is actually needed in vehicular networks. This observation implies that our proposed self-triggered scheme allows much more efficient use of communication bandwidth than the traditional event-triggered methods by providing much larger minimum transmission time interval. The comparison of average transmission time intervals under both triggered schemes is provided in the top-right plot of Fig. 4, which shows that the average interval generated by self-triggered scheme is relatively close to that of the event-triggered one when desired formations are positioned in good channel regions, such as $\alpha_d = 0°, 10°, 20°$. When the desired formation configuration approaches bad channel regions, such as $\alpha_d = 30°, 40°, 50°$, our proposed self-triggered scheme reacts to those formation changes by adaptively adjusting the average transmission time intervals. As shown in the top right plot of Fig. 4, the average transmission time interval decreases to ensure sufficient information updates as the desired formations approach bad channel regions.

Fig. 5 shows the probability distribution of the transmission interval over 100 runs under the proposed self-triggered scheme (top plot) and traditional event-triggered scheme in Wang and Lemmon (2011a) (bottom plot) when the desired formation is in good channel region, $\alpha_d = 0°$. The result shows that even in the good channel region, nearly 30% of the time intervals generated by the event-triggered scheme proposed in Wang and Lemmon (2011a) (top plot in Fig. 5) are below 0.01 s while the percentage of small time intervals below 0.01 s in our proposed self-triggered scheme is 0. This is not surprising since the state-dependent threshold $|e(t)| \leq 0.1591|[\alpha(t) - \alpha_d, L(t) - L_d]|$ in event-triggered scheme, is very sensitive to any small changes on the system states and easy to be violated when they are around the equilibrium.

In this simulation, we are also interested in testing how robust both triggered schemes are against a wide range of fading levels. The robustness of both triggered schemes is evaluated by examining how frequently a small transmission time interval occurs due to channel fading from $\alpha_d = 0°$ to $\alpha_d = 50°$. Fig. 6 shows probability distributions of the transmission time interval lying in each of the intervals $\cup_{i=0}^{9}[i * 0.01, (i+1) * 0.01]$ s under the proposed self-triggered scheme (bottom plot) and event-triggered scheme (top plot). The results show that nearly 30% percent of the time intervals generated by the event-triggered scheme in Wang and Lemmon (2011a) lies in the interval [0, 0.01] s while the percentage generated by the self-triggered scheme in (21) is 0 under all levels of channel fading. This suggests that our proposed self-triggered scheme is more robust against channel fading than traditional event-triggered schemes.

7. Conclusion

This paper developed a novel self-triggered scheme for VNS in the presence of *state-dependent fading channels*. By using a state-dependent fading channel model, the results showed that the proposed self-triggered schemes can achieve efficient use of communication bandwidth with Zeno-free transmission while ensuring four types of *stochastic stability*. Under the proposed self-triggered scheme, this paper also presented a new source coding scheme under which vehicle's states were tracked with performance guarantee even when channel states are time varying and are stochastically changed as a function of vehicle states. Simulation results of a leader–follower example demonstrated that the proposed self-triggered scheme was more efficient in bandwidth utilization and more resilient to deep fading than traditional event-triggered schemes.

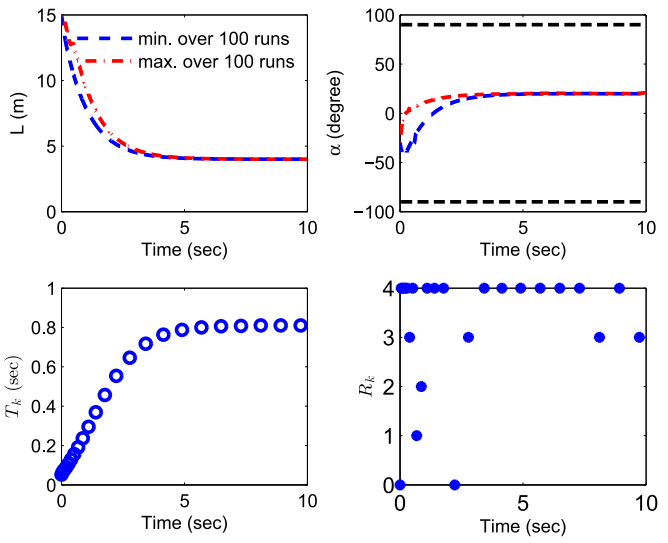

Fig. 3. The maximum and minimum trajectories of $L(m)$ and $\alpha(degree)$ under the self-triggered scheme in (21) (top plots) and one sample of the inter-transmission time interval T_k and number of received bits R_k (bottom plots).

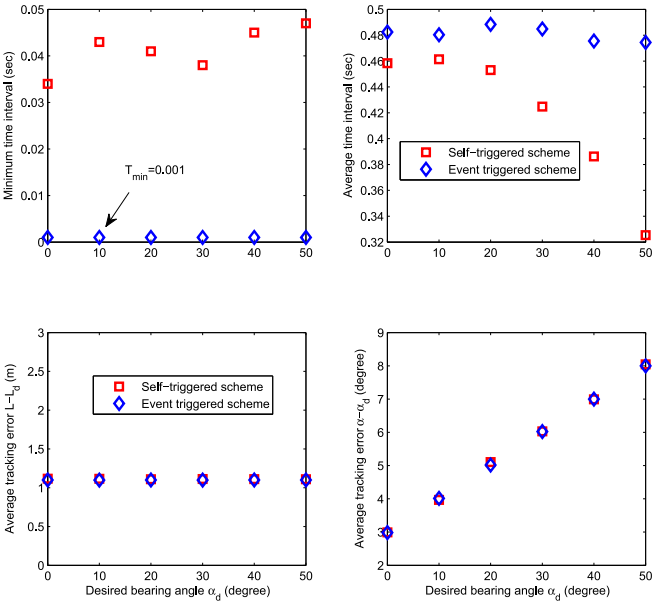

Fig. 4. Comparison of minimum transmission time interval (top left plot), average (top right plot) transmission time intervals and tracking errors in distance (bottom left plot) and bearing angle (bottom right plot) under desired bearing angles $\alpha_d = 0°, 10°, 20°, 30°, 40°, 50°$.

Appendix

Proof of Theorem 8. Let t_k denote the time instant for the kth transmission event and consider the dynamic evolution of the

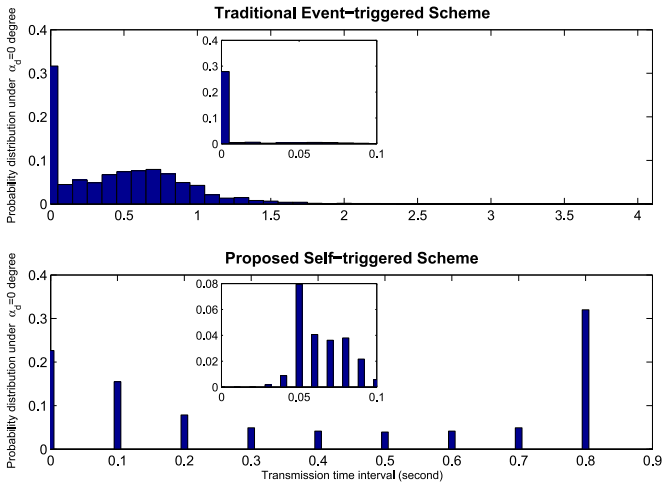

Fig. 5. Distribution of inter-transmission time interval under self-triggered scheme in Theorem 9 and traditional event-triggered scheme (Wang & Lemmon, 2011a).

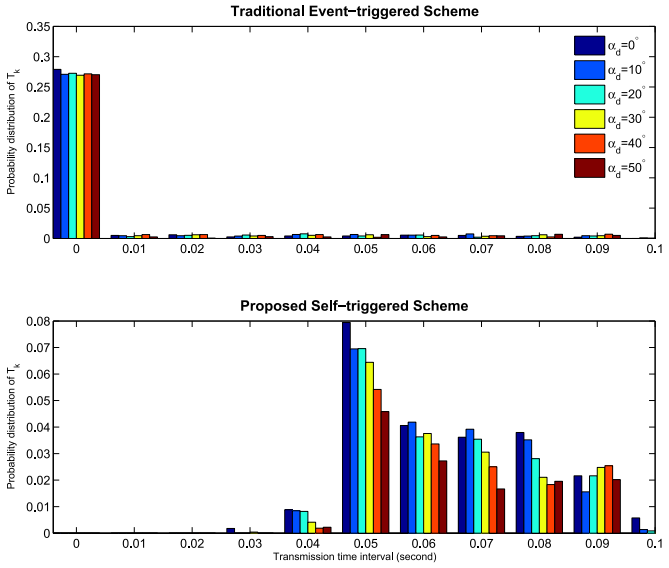

Fig. 6. Distribution of small inter-transmission time intervals under self-triggered scheme in (21) and event-triggered scheme (Wang & Lemmon, 2011a) under desired bearing angles $\alpha_d = 0°, 10°, 20°, 30°, 40°, 50°$.

estimation over the time interval $[t_k, t_{k+1})$. Since Assumption 6 holds, one has $W(e) \leq e^{L_e(t-t_k)}W(e(t_k^+)) + \frac{L_x}{L_e}(e^{L_e(t-t_k)} - 1)|\overline{x}|_{[t_k,t)}$. Since $w_1|e| \leq W(e) \leq w_2|e|$, one further has $|e|_{[t_k,t)} = |e(t)| \leq \frac{w_2}{w_1}e^{L_e(t-t_k)}|e(t_k^+)| + \frac{L_x}{w_1 L_e}(e^{L_e(t-t_k)} - 1)|\overline{x}|_{[t_k,t)}$. Taking the expectation on both sides of the above inequality yields

$$\begin{aligned}
&\mathbb{E}(|e(t)|)\\
&\leq \frac{w_2}{w_1}e^{L_e(t-t_k)}\mathbb{E}(2^{-R(k)})\mathbb{E}(|e(t_k)|) + \frac{L_x(e^{L_e(t-t_k)} - 1)}{w_1 L_e}\mathbb{E}(|\overline{x}|_{[t_k,t)})\\
&\leq \frac{w_2}{w_1}e^{L_e(t-t_k)}G_k\mathbb{E}(|e(t_k)|) + \frac{L_x(e^{L_e(t-t_k)} - 1)}{w_1 L_e}\mathbb{E}(|\overline{x}|_{[t_k,t)})
\end{aligned}$$

where $G_k := G(|x(t_k)|)$. The first inequality holds due to the quantization, $|e(t_k^+)| = 2^{-R_k}|e(t_k)|$ and the fact that the random variable $R(k)$ at time t_k is independent of $e(t_k)$ (before the jump). The second inequality holds because of technical Lemma 7. Suppose the next transmission time instant t_{k+1} is generated by Eq. (21), then one has

$$\begin{aligned}
&\mathbb{E}(|e(t_{k+1})|)\\
&\leq \underbrace{\frac{G_k\frac{w_2}{w_1}(1 + \frac{L_x\overline{\chi}_1}{L_e w_1})}{G_k\frac{w_2}{w_1} + \frac{L_x\overline{\chi}_1}{L_e w_1}}}_{<1}\mathbb{E}(|e(t_k)|) + \underbrace{\frac{L_x}{w_1 L_e}\frac{1 - G_k\frac{w_2}{w_1}}{G_k\frac{w_2}{w_1} + \frac{L_x\overline{\chi}_1}{L_e w_1}}}_{\gamma_{\overline{x}}}\mathbb{E}(|\overline{x}|_{[t_k,t_{k+1})})
\end{aligned}$$

for all $x \in \Omega_x = \{x \in \mathbb{R}^n | G(|x|) < w_1/w_2\}$. Similarly, by Assumption 5, one has $\mathbb{E}(|\overline{x}(t)|) \leq \mathbb{E}(\beta(|\overline{x}(t_k)|, t - t_k)) + \overline{\chi}_1\mathbb{E}(|e|_{[t_k,t)}) \leq \beta(\mathbb{E}(|\overline{x}(t_k)|), t - t_k) + \overline{\chi}_1\mathbb{E}(|e|_{[t_k,t)})$ where the class $\mathcal{KL}$ function $\beta(s, t)$ is concave with respect to s, and thus the second inequality holds due to the Jensen's inequality. It is clear from the representation of $\mathbb{E}(|e(t)|)$ and $\mathbb{E}(|\overline{x}(t)|)$ that the subsystems with states $\mathbb{E}(|e(t)|)$ and $\mathbb{E}(|\overline{x}(t)|)$ are interconnected with linear gains $\gamma_{\overline{x}}$ and $\overline{\chi}_1$. Since

$$\overline{\chi}_1 \cdot \frac{L_x}{w_1 L_e}\frac{1 - G_k\frac{w_2}{w_1}}{G_k\frac{w_2}{w_1} + \frac{L_x\overline{\chi}_1}{L_e w_1}} = \frac{L_x\overline{\chi}_1}{L_e G_k w_2 + L_x\overline{\chi}_1}(1 - G_k\frac{w_2}{w_1}) < 1 \tag{26}$$

and $k \in \mathbb{Z}_{\geq 0}$ is arbitrarily chosen, one knows the system with states $\mathbb{E}(|\overline{x}|)$ and $\mathbb{E}(|e(t)|)$ is asymptotically stable by the small-gain theorem, i.e. $\lim_{t\to\infty}\mathbb{E}(|\overline{x}(t)|) \to 0$. The stability argument is therefore proved.

The Zeno-free transmission generated by Eq. (21) can also be proved by considering that $\forall x \in \Omega_x$

$$\frac{1 - \frac{w_2}{w_1}G(|x|)}{\frac{w_2}{w_1}G(|x|) + \frac{L_x\overline{\chi}_1}{L_e w_1}} > 0 \tag{27}$$

holds. This leads to a strictly positive transmission time interval defined by Eq. (21). Since the function $G(|x|)$ monotonically increases w.r.t. the state $|x|$, then one knows that the function in (27) monotonically decreases w.r.t. $|x|$. Thus, the transmission time interval T generated by (21) monotonically decreases w.r.t. $|x|$. The proof is complete.

Proof of Theorem 9. Following the proof techniques used in Theorem 8, one can obtain that the VNS in (13) is exponentially stable in expectation with respect to origin under the Exp-ISS assumption stated in Assumption 5. Specifically, there must exist an exp-$\mathcal{KL}$ function $\beta(s, t) = c_1\exp(-c_2 t)s$ such that $\forall\overline{x}(0)$, $\mathbb{E}(|\overline{x}(t)|) \leq c_1\exp(-c_2 t)|\overline{x}(0)|, \forall t \in \mathbb{R}_{\geq 0}$. To prove the almost surely asymptotic stability, let $\tau' > \tau \geq 0$ denote any time instant such that $\tau \leq t \leq \tau'$ holds, for any given $\epsilon' > 0$, consider the following probability bound,

$$\begin{aligned}
&\Pr\{\sup_{\tau\leq t<\tau'}|\overline{x}(t)| \geq \epsilon'\} \leq \mathbb{E}\Big\{\sup_{\tau\leq t<\tau'}|\overline{x}(t)|\Big\}/\epsilon'\\
&\leq \mathbb{E}\Big\{\int_\tau^{\tau'}|\overline{x}(t)|dt\Big\}/\epsilon' \leq \int_\tau^{\tau'}\mathbb{E}\Big\{|\overline{x}(t)|\Big\}dt/\epsilon'\\
&\leq \int_\tau^{\tau'}c_1\exp(-c_2 t)|\overline{x}(0)|dt/\epsilon' \leq \frac{c_1|\overline{x}(0)|}{c_2\epsilon'}\left[e^{-c_2\tau} - e^{-c_2\tau'}\right]
\end{aligned} \tag{28}$$

where the first inequality holds due to the Markov inequality and the third inequality holds by exchanging the expectation and integration due to the measurability of the solution process $|\overline{x}(t)|$ and the finiteness of the integral from time τ to τ'. Let $\tau' \to +\infty$, the probability bound in (28) is $\Pr\{\sup_{\tau\leq t}|\overline{x}(t)| \geq \epsilon'\} \leq \frac{c_1|\overline{x}(0)|}{c_2\epsilon'}e^{-c_2\tau} \leq \frac{c_1|\overline{x}(0)|}{c_2\epsilon'}$. Let $\epsilon := \frac{c_1|\overline{x}(0)|}{c_2\epsilon'}$, then there indeed exists a function $\delta(\epsilon, \epsilon') = \frac{c_2\epsilon'}{c_1}$ such that $\Pr\{\sup_{\tau\leq t}|\overline{x}(t)| \geq \epsilon'\} \leq \epsilon$ for any $|\overline{x}(0)| \leq \delta(\epsilon, \epsilon')$. Furthermore, since τ is arbitrarily chosen, consider the following integral

$$\int_0^\infty \Pr\{\sup_{\tau\leq t}|\overline{x}(t)| \geq \epsilon'\}d\tau \leq \int_0^\infty \frac{c_1|\overline{x}(0)|}{c_2\epsilon'}e^{-c_2\tau}d\tau = \frac{c_1|\overline{x}(0)|}{c_2^2\epsilon'}. \tag{29}$$

By the Borel–Cantelli Lemma, the finite integral in (29) implies that $\Pr\{\lim_{\tau\to\infty}\sup_{\tau\le t}|\bar{x}(t)|\ge\epsilon'\}=0$ and then almost surely asymptotic stability defined in (16) holds. The proof is complete.

Proof of Theorem 10. By Assumptions 5 and 6, $\forall t>t_k\in\mathbb{R}_+$, $k\in\mathbb{Z}_+$, one has $\mathbb{E}(|\bar{x}(t)|)\le\beta(\mathbb{E}(|\bar{x}(t_k)|),t-t_k)+\overline{\chi}_1\mathbb{E}(|e|_{[t_k,t)})+\chi_2(M)$ with $|w|_{\mathcal{L}_\infty}\le M$, and

$$\mathbb{E}(|e(t)|)\le\frac{w_2}{w_1}e^{L_e(t-t_k)}G(|x(t_k)|)\mathbb{E}(|e(t_k)|)+\frac{L_wM}{w_1L_e}(e^{L_e(t-t_k)}-1)+\frac{L_x}{w_1L_e}(e^{L_e(t-t_k)}-1)\mathbb{E}(|x|_{[t_k,t)})$$

Since under the self-triggered scheme in (21), the condition in (26) assures that the small-gain theorem holds for the interconnected system of $\mathbb{E}(|\bar{x}(t)|)$ and $\mathbb{E}(|e(t)|)$, the system with states $\bar{X}(t):=[\mathbb{E}(|\bar{x}(t)|);\mathbb{E}(|e(t)|)]$ is then input to state stable with respect to the external disturbance (Jiang & Wang, 2001). In particular, there exist a class $\mathcal{KL}$ function $\beta'(\cdot,\cdot)$ and a class $\mathcal{K}$ function $\chi(\cdot)$ such that $|\bar{X}(t)|\le\beta'(|\bar{X}(0)|,t)+\chi(M)$. Thus, $\forall|\bar{x}_0|\le\Delta_0$, one knows that $\mathbb{E}\{|\bar{x}(t)|\}\le\beta'(\Delta_0,0)+\chi(M)\triangleq\epsilon(M,\Delta_0)$ and $\lim_{t\to+\infty}\mathbb{E}\{|\bar{x}(t)|\}\le\chi(M)$. The proof is complete.

Proof of Theorem 11. Suppose the claim in Theorem 10 holds, for any given $\epsilon>0$, the probability of the system state $\bar{x}$ exiting a given set $\Omega_s=\{\bar{x}\in\mathbb{R}^n||\bar{x}|\le\Delta\}$ at time t can be bounded by $\Pr\{|\bar{x}(t)|\ge\Delta+\epsilon\}\le\frac{\mathbb{E}(|\bar{x}(t)|)}{\Delta+\epsilon}\le\frac{\beta'(\mathbb{E}(|\bar{x}(0)|,t))+\chi(M)}{\Delta+\epsilon}$. The first inequality follows by Markov's Inequality and the second inequality holds due to the *input to state stability*. Taking the limit of time to infinity leads to $\lim_{t\to+\infty}\Pr\{|\bar{x}|\ge\Delta+\epsilon\}\le\frac{\chi(M)}{\Delta+\epsilon}$. Thus, the VNS in (13) with bounded external disturbance is practically stable in probability with the probability bound $\epsilon(M,\Delta)=\frac{\chi(M)}{\Delta+\epsilon}$. The proof is complete.

Proof of Proposition 12. The proof is based on an induction method. Since we assume that the encoder and decoder share the initial value of $\hat{\bar{x}}_0^+$ and U_0^+ and the actual value of initial state $\bar{x}(0)$ lies in the hypercubic box with $\hat{\bar{x}}_0^+$ being its centroid and $2U_0^+$ being its edge length, the case of $k=0$ holds. Next, suppose the case of k holds, i.e., the state $\bar{x}(t_k)$ at time instant t_k lies in the hypercubic box with parameters $(\hat{\bar{x}}_k^+,U_k^+)$ and $|\bar{x}(t_k)-\hat{\bar{x}}_k^+|\le U_k^+$. In the sequel, we show that the case of $(k+1)$th holds under the recursive equations (23a) and (23b).

First, consider the estimation error $e(t):=\bar{x}(t)-(\hat{x}-x^d)=x(t)-\hat{x}$ over time interval $[t_k,t_{k+1}),\forall k\in\mathbb{Z}_{\ge0}$. Let t^- and t^+ denote the time instants before and after the bits are received respectively. By Assumption 6, one has

$$|e(t)|\le\frac{w_2}{w_1}e^{L_e(t-t_k)}|e(t_k^+)|+\frac{L_x}{w_1L_e}(e^{L_e(t-t_k)}-1)|\bar{x}|_{[t_k,t)}+\frac{L_w}{w_1L_e}(e^{L_e(t-t_k)}-1)M \tag{30}$$

Similarly, Assumption 5 leads to

$$|\bar{x}|_{[t_k,t)}\le\beta(|\bar{x}(t_k)|,0)+\overline{\chi}_1|e|_{[t_k,t)}+\chi_2(M) \tag{31}$$

Substituting (31) into (30) and letting $t=t_{k+1}^-$, since $|e(t_{k+1})|=|e(t)|_{[t_k,t)}$, one has $\underbrace{\left(1-\frac{L_x\overline{\chi}_1}{w_1L_e}(e^{L_eT_k}-1)\right)}_{\eta_{k+1}}|e(t_{k+1}^-)|\le\frac{w_2}{w_1}e^{L_eT_k}|e(t_k^+)|+\frac{e^{L_eT_k}-1}{w_1L_e}\Big(L_x\beta(|\bar{x}(t_k)|,0)+L_wM+L_x\chi_2(M)\Big)$. Since the transmission sequence $\{t_k\}$ is generated by (21) and the small-gain condition (26) holds, $\eta_k>0,\forall k\in\mathbb{Z}_+$. Suppose $|e(t_k^+)|\le U_k^+$, then the following inequality

$$|e(t_{k+1}^-)|\le\frac{1}{\eta_{k+1}}\left(\frac{w_2}{w_1}e^{L_eT_k}U_k^++\frac{e^{L_eT_k}-1}{w_1L_e}\left(L_x\beta(|\hat{\bar{x}}_k^+|+U_k^+,0)+L_wM+L_x\chi_2(M)\right)\right):=U_{k+1} \tag{32}$$

holds due to $\eta_k>0$ and $|\bar{x}(t_k)|\le|\hat{\bar{x}}_k^+|+U_k^+$. Upon successfully receiving R_{k+1} blocks of bits at time t_{k+1}^+, one has $|e(t_{k+1}^+)|\le2^{-R_{k+1}}|e(t_{k+1}^-)|$. Let $U_{k+1}^+:=\frac{2^{-R_{k+1}}}{\eta_{k+1}}\left(\frac{w_2}{w_1}e^{L_eT_k}U_k^++\frac{e^{L_eT_k}-1}{w_1L_e}\left(L_x\beta(|\hat{\bar{x}}_k^+|+U_k^+,0)+L_wM+L_x\chi_2(M)\right)\right)$, then $|e(t_{k+1}^+)|\le U_{k+1}^+$. Since the transmission time interval $[t_k,t_{k+1}]$ is selected arbitrarily, $\{U_k^+\}$ is a sequence of upper bounds on the estimation errors $\{e(t_k^+)\}$, i.e., $|\bar{x}(t_k)-\hat{\bar{x}}_k^+|\le U_k^+,\forall k\in\mathbb{Z}_{\ge0}$.

Secondly, the state estimate $\hat{\bar{x}}_{k+1}^+$ is updated by selecting the centroid of an updated hypercubic box that contains $\bar{x}(t_{k+1})$. To be specific, during the time interval $[t_k,t_{k+1})$, the centroid $\hat{\bar{x}}(t)$ of the hypercubic box is updated by both encoder and decoder according to the dynamic equation $\dot{\hat{\bar{x}}}=f_{\bar{x}}(\bar{x},0,0)$ with initial value $\hat{\bar{x}}_k^+$. The centroid of the expanded hypercubic box at time instant t_{k+1}^- before receiving new information bits, is $\Phi(\hat{\bar{x}}(t_k),T_k):=\hat{\bar{x}}(t_{k+1}^-)=\hat{\bar{x}}_k^++\int_{t_k}^{t_k+T_k}f_{\bar{x}}(\hat{\bar{x}},0,0)dt$. By inequality (32), one knows that the state $\bar{x}(t_{k+1})$ is guaranteed to lie in an expanded hypercubic box with the centroid $\hat{\bar{x}}(t_{k+1}^-)$ and the size U_{k+1}. Upon receiving R_{k+1} blocks of bits at time instant t_{k+1}, the expanded hypercubic box is partitioned into $2^{nR_{k+1}}$ number of sub-boxes with each sub-box's centroid being encoded by a binary sequence $\{b_j\}_{j=1}^{R_{k+1}}$. Thus, for a given centroid $\Phi(\hat{\bar{x}}(t_k),T_k)$, a given box length U_{k+1} and $\{b_j\}_{j=1}^{R_{k+1}}$, the function $q(b_{ji})\in\{-1,1\}$ decodes the ith bit in the jth block as a relative "position" to the centroid $\Phi(\hat{\bar{x}}(t_k),T_k)$. By a uniform quantization method (Martins et al., 2006), the centroid of the sub-box that contains the actual state $\bar{x}(t_{k+1})$ is thus $\hat{\bar{x}}_{k+1}^+=U_{k+1}\sum_{j=1}^{R_{k+1}}\frac{1}{2^j}q\big(b_j(k+1)\big)+\Phi(\hat{\bar{x}}_k^+,T_k)$. The proof is complete.

References

Abdelrahim, M., Dolk, V., & Heemels, W. (2016). Input-to-state stabilizing event-triggered control for linear systems with output quantization. In *2016 IEEE 55th conference on decision and control* (pp. 483–488). IEEE.

Abdelrahim, M., Postoyan, R., Daafouz, J., & Nešić, D. (2016). Stabilization of nonlinear systems using event-triggered output feedback controllers. *IEEE Transactions on Automatic Control*, *61*, 2682–2687.

Akki, A. S. (1994). Statistical properties of mobile-to-mobile land communication channels. *IEEE Transactions on Vehicular Technology*, *43*, 826–831.

Akyildiz, I. F., Pompili, D., & Melodia, T. (2005). Underwater acoustic sensor networks: research challenges. *Ad Hoc Networks*, *3*, 257–279.

Anderson, R. P., Milutinović, D., & Dimarogonas, D. V. (2015). Self-triggered sampling for second-moment stability of state-feedback controlled sde systems. *Automatica*, *54*, 8–15.

Balanis, C. A. (2016). *Antenna theory: Analysis and design*. John Wiley & Sons.

Borgers, D. N., & Heemels, W. M. (2014). Event-separation properties of event-triggered control systems. *IEEE Transactions on Automatic Control*, *59*, 2644–2656.

Cheng, L., Henty, B. E., Stancil, D. D., Bai, F., & Mudalige, P. (2007). Mobile vehicle-to-vehicle narrow-band channel measurement and characterization of the 5.9 ghz dedicated short range communication (dsrc) frequency band. *IEEE Journal on Selected Areas in Communications*, *25*, 1501–1516.

Choudhury, R. R., Yang, X., Ramanathan, R., & Vaidya, N. H. (2002). Using directional antennas for medium access control in ad hoc networks. In *Proceedings of the 8th annual international conference on mobile computing and networking* (pp. 59–70). ACM.

Dolk, V., Borgers, D. P., & Heemels, W. (2017). Output-based and decentralized dynamic event-triggered control with guaranteed $\mathcal{L}_p$-gain performance and zeno-freeness. *IEEE Transactions on Automatic Control*, *62*, 34–49.

Dolk, V., & Heemels, M. (2017). Event-triggered control systems under packet losses. *Automatica*, *80*, 143–155.

Dolk, V. S., Ploeg, J., & Heemels, W. M. H. (2017). Event-triggered control for string-stable vehicle platooning. *IEEE Transactions on Intelligent Transportation Systems*, *18*, 3486–3500.

Goldsmith, A. J., & Chua, S.-G. (1997). Variable-rate variable-power mqam for fading channels. *IEEE Transactions on Communications*, *45*, 1218–1230.
Gommans, T., Antunes, D., Donkers, T., Tabuada, P., & Heemels, M. (2014). Self-triggered linear quadratic control. *Automatica*, *50*, 1279–1287.
Guinaldo, M., Lehmann, D., Sanchez, J., Dormido, S., & Johansson, K. H. (2012). Distributed event-triggered control with network delays and packet losses. In *2012 IEEE 51st annual conference on decision and control* (pp. 1–6). IEEE.
Guo, G., & Wang, L. (2014). Control over medium-constrained vehicular networks with fading channels and random access protocol: a networked systems approach. *IEEE Transactions on Vehicular Technology*, *64*, 3347–3358.
Guo, G., & Wen, S. (2015). Communication scheduling and control of a platoon of vehicles in vanets. *IEEE Transactions on Intelligent Transportation Systems*, *17*, 1551–1563.
Heemels, W., Donkers, M., & Teel, A. R. (2013). Periodic event-triggered control for linear systems. *IEEE Transactions on Automatic Control*, *58*, 847–861.
Heemels, W., Johansson, K. H., & Tabuada, P. (2012). An introduction to event-triggered and self-triggered control. In *2012 IEEE 51st IEEE conference on decision and control* (pp. 3270–3285). IEEE.
Hetel, L., Fiter, C., Omran, H., Seuret, A., Fridman, E., Richard, J.-P., & Niculescu, S. I. (2017). Recent developments on the stability of systems with aperiodic sampling: An overview. *Automatica*, *76*, 309–335.
Hu, B., & Lemmon, M. D. (2013). Using channel state feedback to achieve resilience to deep fades in wireless networked control systems. In *Proceedings of the 2nd international conference on high confidence networked systems*.
Hu, B., & Lemmon, M. D. (2014). Event triggering in vehicular networked systems with limited bandwidth and deep fading. In *2014 53rd IEEE conference on decision and control* (pp. 3542–3547). IEEE.
Hu, B., & Lemmon, M. D. (2015). Distributed switching control to achieve almost sure safety for leader-follower vehicular networked systems. *IEEE Transactions on Automatic Control*, *60*, 3195–3209.
Jiang, Z.-P., & Wang, Y. (2001). Input-to-state stability for discrete-time nonlinear systems. *Automatica*, *37*, 857–869.
Kozin, F. (1969). A survey of stability of stochastic systems. *Automatica*, *5*, 95–112.
Kurose, J. F. (2005). *Computer networking: A top-down approach featuring the internet* (3rd ed.). Pearson Education India.
Lehmann, D., & Lunze, J. (2012). Event-based control with communication delays and packet losses. *International Journal of Control*, *85*, 563–577.
Li, H., Chen, Z., Wu, L., & Lam, H.-K. (2016). Event-triggered control for nonlinear systems under unreliable communication links. *IEEE Transactions on Fuzzy Systems*.
Li, L., Wang, X., & Lemmon, M. D. (2017). Efficiently attentive event-triggered systems with limited bandwidth. *IEEE Transactions on Automatic Control*, *62*, 1491–1497.
Martins, N. C., Dahleh, M. A., & Elia, N. (2006). Feedback stabilization of uncertain systems in the presence of a direct link. *IEEE Transactions on Automatic Control*, *51*, 438–447.
Mazo, M., & Tabuada, P. (2008). On event-triggered and self-triggered control over sensor/actuator networks. In *2008 47th IEEE conference on decision and control* (pp. 435–440). IEEE.
Mecklenbrauker, C. F., Molisch, A. F., Karedal, J., Tufvesson, F., Paier, A., Bernadó, L., Zemen, T., Klemp, O., & Czink, N. (2011). Vehicular channel characterization and its implications for wireless system design and performance. *Proceedings of the IEEE*, *99*, 1189–1212.
Molisch, A. F., Tufvesson, F., Karedal, J., & Mecklenbrauker, C. F. (2009). A survey on vehicle-to-vehicle propagation channels. *IEEE Wireless Communication*, *16*, 12–22.
Nešić, D., & Teel, A. R. (2004). Input–output stability properties of networked control systems. *IEEE Transactions on Automatic Control*, *49*, 1650–1667.
Papadimitratos, P., De La Fortelle, A., Evenssen, K., Brignolo, R., & Cosenza, S. (2009). Vehicular communication systems: Enabling technologies, applications, and future outlook on intelligent transportation. *IEEE Communications Magazine*, *47*, 84–95.
Park, P., Khadilkar, H., Balakrishnan, H., & Tomlin, C. J. (2014). High confidence networked control for next generation air transportation systems. *IEEE Transactions on Automatic Control*, *59*, 3357–3372.
Peng, C., & Yang, T. C. (2013). Event-triggered communication and $\mathcal{H}_\infty$ control co-design for networked control systems. *Automatica*, *49*, 1326–1332.
Stüber, G. L. (2011). *Principles of mobile communication*. Springer Science & Business Media.
Swaroop, D., & Hedrick, J. K. (1996). String stability of interconnected systems. *IEEE Transactions on Automatic Control*, *41*, 349–357.
Tabuada, P. (2007). Event-triggered real-time scheduling of stabilizing control tasks. *IEEE Transactions on Automatic Control*, *52*, 1680–1685.
Tallapragada, P., & Chopra, N. (2012). Event-triggered dynamic output feedback control for lti systems. In *2012 IEEE 51st Annual conference on decision and control* (pp. 6597–6602). IEEE.
Tanner, H. G., Pappas, G. J., & Kumar, V. (2004). Leader-to-formation stability. *IEEE Transactions on Robotics and Automation*, *20*, 443–455.
Tatikonda, S., & Mitter, S. (2004). Control under communication constraints. *IEEE Transactions on Automatic Control*, *49*, 1056–1068.
Tomlin, C. J., Lygeros, J., & Sastry, S. S. (2000). A game theoretic approach to controller design for hybrid systems. *Proceedings of the IEEE*, *88*, 949–970.
Tse, D., & Viswanath, P. (2005). *Fundamentals of wireless communication*. Cambridge University Press.
Wang, X., & Lemmon, M. D. (2009). Self-triggered feedback control systems with finite-gain $\mathcal{L}_2$ stability. *IEEE Transactions on Automatic Control*, *54*, 452–467.
Wang, X., & Lemmon, M. (2011). Attentively efficient controllers for event-triggered feedback systems. In *2011 50th IEEE conference on decision and control and european control conference* (pp. 4698–4703). IEEE.
Wang, X., & Lemmon, M. D. (2011). Event-triggering in distributed networked control systems. *IEEE Transactions on Automatic Control*, *56*, 586–601.
Wong, W. S., & Brockett, R. W. (1999). Systems with finite communication bandwidth constraints. ii. stabilization with limited information feedback. *IEEE Transactions on Automatic Control*, *44*, 1049–1053.
Wu, B., Lin, H., & Lemmon, M. (2014). Formal methods for stability analysis of networked control systems with ieee 802.15 4 protocol. In *2014 IEEE 53rd annual conference on decision and control* (pp. 5266–5271). IEEE.
Yu, H., & Antsaklis, P. J. (2013). Event-triggered output feedback control for networked control systems using passivity: Achieving l2 stability in the presence of communication delays and signal quantization. *Automatica*, *49*, 30–38.
Zhang, W., Branicky, M. S., & Phillips, S. M. (2001). Stability of networked control systems. *IEEE Control Systems*, *21*, 84–99.
Zhang, Q., & Kassam, S. A. (1999). Finite-state markov model for rayleigh fading channels. *IEEE Transactions on Communications*, *47*, 1688–1692.

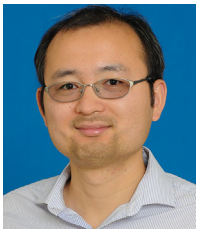

Bin Hu received the M.S. degree in control and system engineering from Zhejiang University, Hangzhou, China, in 2010 and the Ph.D. degree from The University of Notre Dame, Notre Dame, IN, USA, in 2016. He is currently Assistant Professor in the department of engineering technology at Old Dominion University, Norfolk, VA, USA. His research interests include networked control systems, cybersecurity, distributed control and optimization, and human machine interaction.